NTNU

Norwegian University of
Science and Technology

Improved Version of Energy Efficient Motor for Shell Eco Marathon

Half Weight with Higher Efficiency

Lubna Nasrin

Master of Science in Electric Power Engineering

Submission date: November 2011

Supervisor: Robert Nilssen, ELKRAFT

Co-supervisor: Juliette Soulard, KTH. Sweden

Norwegian University of Science and Technology
Department of Electric Power Engineering

Table of Contents

Abstract

The goal of the thesis is to analyze an existing Axial Flux Permanent Magnet motor used for Shell Eco Marathon from the Norwegian University of Science and Technology (NTNU). The existing machine has been analysed and modified to achieve improved power density at high efficiency with lowered weight.

A detailed literature study on AFPM machine topologies, winding and magnet arrangements is covered. The magnet arrangement of the existing machine has been transformed from conventional North-South to Halbach array.

The preliminary analytical calculations were done by using analytical expressions. After that, for an improved design, an efficiency-based optimization has been used to improve the obtained parameters from analytical calculation. This optimization has been performed with the help of *fmincon* solver in the Matlab optimization tool. The optimized values after being compared with the analytical calculation, has been used to run Finite Element Method simulations.

The new design with optimum performance parameters displays an improvement of overall efficiency with decreased weight in comparison. The new machine has a 97.2% efficiency and weights only 6.24 kg. In comparison with the existing machine, the weight of the new machine is almost half with improved efficiency.

Keywords

Axial Flux, Permanent Magnet, Synchronous Motor, Ironless Stator, Halbach.

Chapter 1 Introduction

1.1 Background

Shell Eco Marathon is a racing competition, which provides a platform for building up high efficiency vehicles developed by Master students. The traction motor of the vehicle must show a combination of highest possible efficiency with lowest weight since it is used in a tough competition environment (racing challenge). The efficiency should be maximized considering the power speed range so that the car should be able to run at its highest performance under all conditions.

For the last few years, the Norwegian University of Science and Technology (NTNU) team is participating in Shell Eco Marathon competition on basis of the urban concept '*Fuel cell*'. For the upcoming year design, the team has decided to improve the performance of the existing traction motor. The machine to be improved is a 102 W, 275 rpm motor and has an efficiency of 94% with a weight of 12Kg.

Figure 1 shows the Norwegian University of Science and Technology (NTNU) vehicle from 2010 for the Shell Eco Marathon competition.

Fig 1: DNV fuel fighter

1.2 Goal of the Thesis

The goal of the new design of the traction motor is to minimize the electrical and mechanical losses in the machine thus maximizing the overall efficiency. Reducing the electrical losses by small amount may greatly increase the possibility of winning the competition. To avoid losses in the mechanical gearbox, the machine was already designed as a direct drive system.

The purpose of this thesis work was first to analyze the parameters affecting machine efficiency. Possible changes of topologies were to be examined before and hence optimizing the parameters to maximize efficiency. A comparison between the performance parameters of the existing design and optimized design should also be made.

Building of high performance motors for racing competition is usually very expensive. While designing the machine, cost was not taken as a constraint.

1.3 Contents of the Report

The report has the following structure:

Chapter 2 presents the theory of the ironless axial flux permanent magnet machine (AFPM). Arrangement of magnet and stator winding is discussed in detail. Individual components of AFPM for e.g. twin rotor, ironless stator etc. are also discussed briefly. Description regarding the construction of the machine i.e a direct driven, in wheel is also presented in this chapter.

Chapter 3 describes the design requirements and constraints regarding the existing motor. Analytical calculation and optimization of parameters leading to optimum value of desired performance parameters with the help of Matlab Optimization tool are investigated in detail.

Chapter 4 contains the design procedure of the optimized machine in FEM. The step-by-step design procedure, adaptation in COMSOL 4.1 and FEM simulations are discussed. The comparison in between of the results of the FEM simulations and analytical calculation has also been discussed.

Chapter 5 presents conclusions and design improvement suggestions.

Chapter 2 Theory

2.1 Background

In recent years, permanent magnet brushless machines have received a lot of attention for having high power density and high efficiency.

Axial Flux Permanent Magnet (AFPM), also known as disc type machine follows the same rule of electromagnetic design as Radial Flux Permanent Magnet (RFPM). However, the mechanical design and assembly process are different and more complex.

In AFPM, the magnetic flux is generated axially along the axis of the rotor whereas in RFPM, the magnetic flux transverses radially the airgap. Figure 2 and 3 display the flux and current direction of RFPM and AFPM.

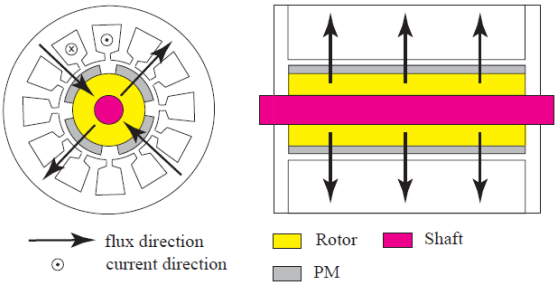

Fig 2: Flux and current directions of RFPM [3]

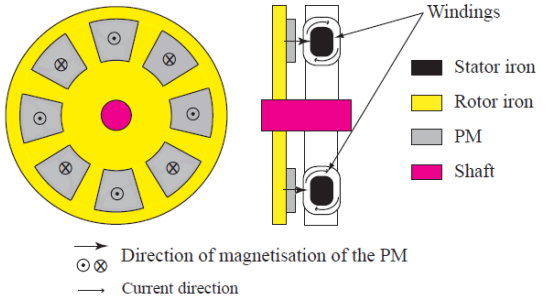

Fig 3: Flux and current directions of AFPM [3]

AFPM is more attractive for having pancake shape. Its compact construction allows utilization of the large radius, which results in maximum torque generation. High moment of inertia, which appears for large rotor diameter can be developed for in wheel machines. However, this is a drawback for the considered application.

The existing machine was designed with Axial Flux Permanent Magnet (AFPM) for having potential advantages over RFPM [2]. This chapter evaluates each component of the machine with its advantages and disadvantages.

2.2 AFPM Topologies

The advantage of AFPM is larger outer diameter and shorter axial length in comparison to RFPM. This type of machine can easily be fit inside the wheel.

From construction point of view [1, 11], the different configurations of AFPM are shown below:

- Single sided AFPM
- Double sided AFPM
- Multi disc AFPM

All three AFPM machines can be designed either with slotted stator or with slotless stator.

The single sided AFPM machine having single sided permanent magnet with coreless stator has low torque production capability. This is the simplest construction, which has no axial force in between of the stator and rotor. A typical representation of single sided AFPM is shown in figure 4.

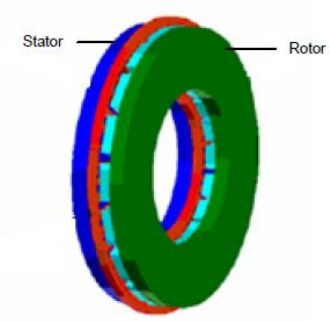

Fig 4: Single sided AFPM [5]

The low torque production capability can be overcomed by enlarging the motor diameter. However, the double disc motor can be a better solution if torque density is an issue. The double disc motor can be designed either as twin rotor or twin stator. Double stator design requires more stationary iron. For this reason, twin rotor design is more preferable to avoid excess eddy current loss.

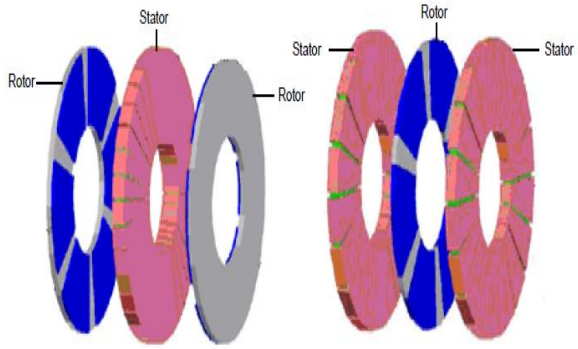

Fig 5: Double sided AFPM (interior stator to the left, interior rotor to the right) [5]

One way of placing the permanent magnets in the rotor disk is by surface mounting the magnets with glue on the rotor surface. Another way is to embed the magnet inside the rotor disk. In many cases, surface mounted permanent magnet is preferable if manufacturing cost of the machine is low. Figure 6 and 7 present the different possible magnet placements.

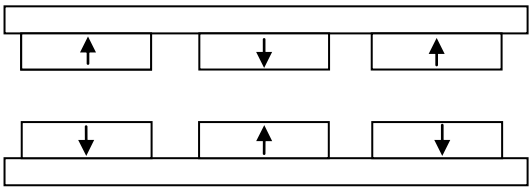

Fig 6: Surface mounted permanent magnets

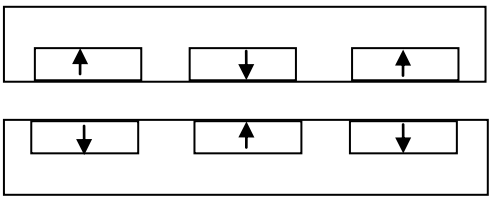

Fig 7: Embedded permanent magnets

The reasons for choosing AFPM instead of RFPM are:

- The AFPM machine is more preferable when design requirements as high power density exists.
- The inner diameter of the AFPM is greater than the shaft diameter, which gives better ventilation.
- AFPM is a suitable choice for low speed operation due to its larger outer diameter of the core and high number of poles.

It would be difficult to accomodate the axial part of the end winding if a RFPM design was chosen due to the reduced space in this application. A really high pole number could help but it would imply a higher frequency, not suitable when high efficiency is looked for. Therefore, RFPM design was not taken into consideration.

2.3 Number of Poles

Number of poles is an important factor when designing a AFPM machine. For low speed operation, higher number of poles is more preferable. AFPM machines have short axial

length. A high number of poles reduces the endwinding length, requiring even less space axially. However, it increases the eddy current loss in the stator winding.

From practical point of view, number of poles can be increased within limits such that the dimensions of the poles are not too small. This would result in increasing complexity during assembly of the poles on the rotor.

2.4 Coreless Stator

The major advantage of coreless stator [1, 12] is negligible axial forces in between of stator and rotor. In practice, coreless stator coils are placed in a moulded structure. This configuration eliminates use of ferromagnetic material such as steel laminations or SMC powder, thus reducing core losses, (i.e. hysteresis losses and eddy current losses). For this reason, this type of machine provides higher efficiency without cogging torque compared to the conventional ones. The mass of the machine is also reduced at given air gap flux density. However, larger volume of PM material is used to achieve required air gap flux density. The stator winding has been sandwiched in between twin rotors. This two opposing rotor disks generate the airgap magnetic field as well as a high attractive force. Significant eddy current losses in stator winding may occur as the flux passes through the copper while operating at relatively high frequency. The electromagnetic torque can be derived on the basis of Lorentz force theorem.

Construction and assembly of coreless stator is comparatively more difficult than the slotted stator. The winding of coreless stator is mould into epoxy resin and hardener. This resin performs in a similar way mechanically as laminated stator core. Cooling of the machine should also be taken in consideration. It is a drawback of ironless stator to cool away losses with difficulty. However, thermal analysis has not been considered for this design.

2.5 Winding Layout

The winding topologies of electrical machines are:

- Distributed winding
- Concentrated winding

The most common stator winding layout for RFPM is distributed winding. With this winding topology, it is required that the end winding of the phase coil overlaps each other. This creates a larger end winding. In recent studies, concentrated winding layout has received some attention since it does not require the overlapping of the end windings. The main advantage of non-overlapping concentrated winding is shorter axial length of the machine due to shorter end winding length. With non-overlapping concentrated winding, the copper loss may be reduced as the volume of copper used in the stator winding is reduced.

For coreless AFPM, it is desirable to have non-overlapping winding. Shorter axial length is one of the properties of AFPM. Therefore, using overlapping winding layout will not be suitable for this case due to larger end winding length. Figure 8 and 9 present the layout of an overlapping winding and non- overlapping winding respectively.

Fig 8: Overlapping winding layout [4]

Overlapping winding layout has the winding factor of 1 in one slot per pole per phase configurations. The coil pitch and pole pitch are equal.

Fig 9: Non-overlapping winding layout [4]

Non-overlapping winding layout has a lower winding factor since the pole pitch and coil pitch are not equal. To increase the winding factor, fractional values of slot per pole per phase are used.

In case of trapezoidal shaped coil configuration, the end winding of the coils are manufactured by bending the end winding upwards and downwards respectively. The ends of the coils are bend with a certain angle so that the active conductors lie in the same plane, which places the end winding close together.

Figure 10 displays a typical trapezoidal coil shape.

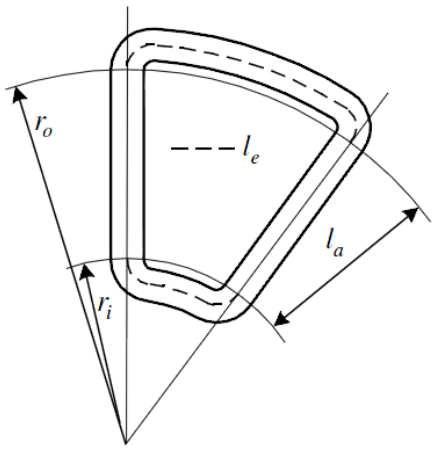

Fig 10: Trapezoidal coil shape [4]

Another coil outline of AFPM is rhomboidal coil. The advantage of using this coil configuration is to have shorter end winding length. Reducing the length of the machine also reduces the volume of copper used in the machine. Therefore, it results the reduction of copper loss of the machine. [9]

The disadvantage of this type of winding topology is the reduction of the torque. This can be overcomed by opting for higher number of poles.

The existing machine was designed with double layer wave winding. To reduce the eddy current losses of the machine, the winding is made with Litz wire.

Figure 11 represents the design of the existing machine of a three-phase wave winding with all the connection points and phase sequences.

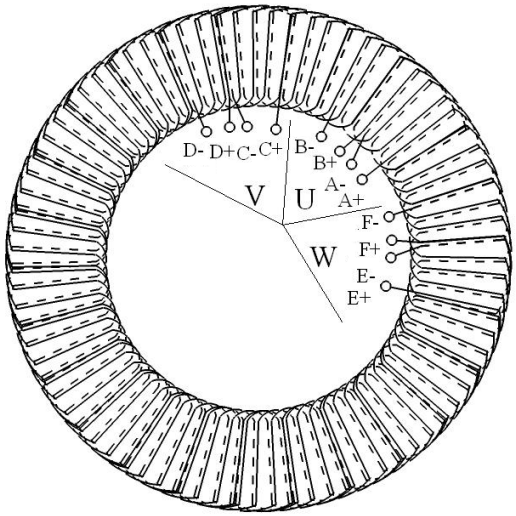

Fig 11: Three phase wave winding with all connection points and phase sequences [2]

The 12 connections can be connected in either series or parallel. When the car is at higher speed, the winding of the machine can be connected in parallel to increase the speed range. While the machine is in accelerating mode, the windings are to be connected in series. Figure 12 and figure 13 represent the series and parallel connections of the winding arrangement correspondingly.

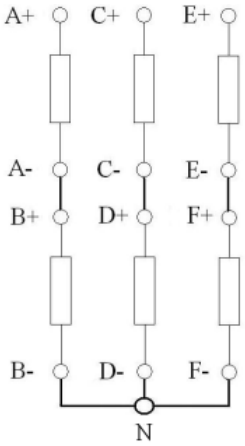

Fig 12: Double layer wave winding connection connected in series [2]

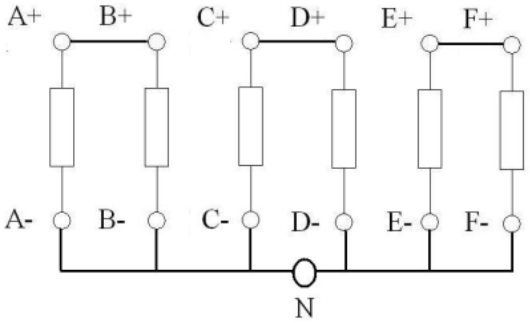

Fig 13: Double layer wave winding connection connected in parallel [2]

Construction with Litz wire reduces the eddy current loss of the machine, therefore, increases the efficiency. However, using Litz wire is more expensive than traditional copper wire.

2.6 Magnet Arrangement

Two types of magnet arrangements can be used for this design. One is conventional single N-S array and the other one is Halbach arrangement. In both cases, rare earth magnet NdFeB is used. Figure 14 and 15 display the typical magnet arrangements.

The existing machine was designed with conventional N-S array. This arrangement is less expensive and simpler to build up.

This type of magnet arrangement requires more back iron, which increases the weight of the machine.

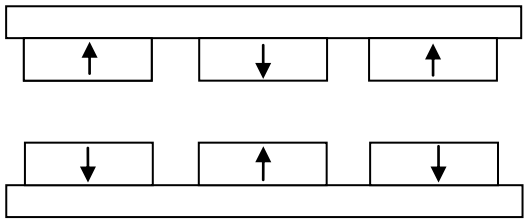

Fig 14: Conventional N-S array

The key concept of the Halbach array is that the magnetization vector of PMs should rotate as a function of distance along the array.

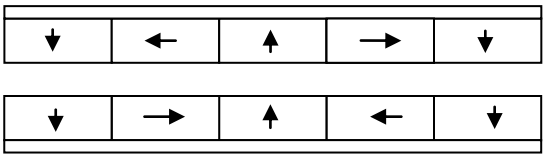

Fig 15: Halbach array (90^0 arrangement)

Halbach arrangement of PM gives more sinusoidal magnetic field than the conventional array. No ferromagnetic material is required. The PM material can be glued with any supporting structure of plastic or aluminum. This is one of the major reasons for having lowered weight of the machine. Also, lower distortion is possible with this magnet arrangement. The PMs can be arranged with 45^0, 60^0 and 90^0 Halbach array. For 90^0 arrangement, the number of PM pieces per wavelength is n_m = 4, whereas n_m =6 for 60^0 and n_m =8 for 45^0 arrangement.

Among the drawbacks for this type of design, expense and complexity in manufacturing are the significant factors.

Chapter 3 Analytical Calculation Regarding Machine Design

3.1 Background and Specification

The goal of this analysis was to obtain parameters leading to improved performance of the existing machine. Improved performance corresponds to higher efficiency with lowered weight of the machine in this application.

In this chapter, the choice of machine parameters and analytical calculations were described respectively.

The design criteria were based on Shell Eco Marathon rules [14] and previous year design information [2]. The design choices for the existing machine were:

- AFPM for shorter axial motor length.
- Ironless stator to eliminate iron losses.
- Double layer wave winding with Litz wire for reducing eddy current losses.

The only change made in the design of the existing machine was the modification of the magnet arrangement. Previously, conventional NS arrangement with NdFeB permanent magnet was used. Now, it was suggested to work with the Halbach arrangement, as it does not require back iron. A reduced weight of the machine is the expected outcome.

The specified design parameters are shown in table 3.1.

Parameter	Value
Nominal torque	3.5 Nm
Nominal speed	275 rpm
Supplied voltage	30-48 V
Induced voltage, E_f	20-30V
Speed in Km/h	25
Efficiency	As high as possible
Weight	As low as possible

Table 3.1 Specified design characteristics

All the design equations of this project and presented in this report as equ 3.1 to equ 3.17 were taken from the axial flux permanent magnet brushless machine book [1]. Initially, Matlab scripts were developed to check the performance of the machine and obtain an initial design. Matlab optimization tool was used in a second step to acquire the optimum point of varying parameters. Finally, the analytical results were verified by FEM analysis. Here, COMSOL Multiphysics 4.1 was used for this purpose.

3.2 Sizing of the Machine

The motor has to be positioned inside the left rear wheel. It depends on the maximum diameter of the rim, which is 340 mm. The maximum stator diameter, set as 330 mm in previous year design, was kept unchanged. The value of the outer diameter of the rotor was also kept unchanged. It equals to 315 mm.

3.3 Magnetic Design

The existing machine was designed for having sinusoidal magnetic field. Sinusoidal flux reduces the harmonic distortion of voltage, which results in less harmonic losses.

Now the goal of this design is to have a strong sinusoidal magnetic flux density with lowered weight of the machine. For this purpose, Halbach magnet arrangement was used to

reduce the weight of the machine as PM is arranged without any ferromagnetic core. In case of Halbach arrangement, the power efficiency of the machine is doubled since the fundamental field is 1.4 times stronger than the conventional arrangement of the magnet [1]. Magnetic saturation does not exist since there is no use of steel magnetic circuit in the rotor or stator.

The flux passes through the PM material to airgap. Thus, magnetic flux equals to,

$$\phi_f = \frac{1}{8p}\alpha_i B_{mg}\pi D_o^2(1-k_D^2) \qquad \text{equ 3.1}$$

The peak value of the magnetic flux density at the active surface of the magnet can be calculated by using equ 3.2.

$$B_{mo} = B_r[1-\exp(-\beta h_m)]\frac{\sin(\pi/n_M)}{(\pi/n_M)}$$

equ 3.2

Where,

B_r is the remanent flux density of the magnet.

n_M is the number of PM pieces per wavelength.

$\beta = 2\pi/l_a$, where, l_a is the spatial period of the wavelength.

The magnetic flux density in between the disc for the double-sided configuration with Halbach array can be expressed as,

$$B_z(x,z) = B_{mo}\sin(\beta x)\frac{1}{\cosh\left(\beta\frac{t}{2}\right)}\cosh(\beta z)$$

equ 3.3

Here, t is the magnet-to-magnet distance.

The results obtained with the help of equation stated above, have been verified with FEM. In this case, COMSOL 4.1 was used for verifying the result.

3.4 Electromagnetic Torque:

The average electromagnetic torque of the AFPM was calculated by the following expression:

$$T_d = \frac{1}{4}\alpha_i m_1 N_1 k_{w1} B_{mg} D_{out}^2(1-k_D^2) I_a$$

equ 3.4

$$Diameter\ ratio, k_D = \frac{D_{in}}{D_{out}}$$

$$k_T = \frac{m_1}{\sqrt{2}} p N_1 k_{w1}\phi_f \qquad \text{equ 3.5}$$

Electromechanical torque can be expressed as a function of diameter ratio. For a given outer diameter, the maximum value for torque is obtained by $k_D = \frac{1}{\sqrt{3}}$ [8,9]. However, in practice, it is not possible to obtain maximum torque with $k_D = \frac{1}{\sqrt{3}}$. Initially, the diameter ratio was chosen 0.65, which gives the value of inner diameter of the rotor ring to 205 mm (approximate) [2]. In addition, this parameter has been optimized later to have the optimum value according the project specifications.

3.5 Electrical Design

Induced Voltage:

In the previous design, the back emf of the motor was set equal to the voltage, which is delivered by the fuel cell [2]. The induced voltage constant, K_E of the machine was considered to be 0.083 V/rpm.

Number of Turns:

The induced voltage has a major influence on the number of turns of the machine. The

number of slots per pole per phase is set to 1 for full pitch winding layout. In coreless machine, physically stator slot does not exist. The term slot is replaced by ''coil side'' for this type of machine.

$q_1 = 1$

$s_1 = q_1 * (2p) * m_1$

Where, S_1 is the number of single layer coil sides, which is equivalent to the number of slots.

The distribution-winding factor,

$$k_{d1} = \frac{\sin\left(\pi/2m_1\right)}{q_1 * \sin\left[\pi/(2 * m_1 * q_1)\right]}$$

The pitch-winding factor,

$$k_{p1} = \sin\left(\beta\frac{\pi}{2}\right)$$

The winding factor,

$k_{w1} = k_{p1} * k_{d1}$

Thus, the number of turns per phase of the machine can be expressed as,

$$N_1 = \frac{k_E}{\sqrt{2}\pi p k_{w1}\phi_f} \qquad \text{equ 3.6}$$

Where, k_E = EMF constant

Stator Dimension:

The stator width should be chosen in such a way so that there should be sufficient space to accommodate the number of turns.

The maximum width of the stator can be expressed by,

$$w_s = \frac{\pi D_i}{s_1} \qquad \text{equ 3.7}$$

3.6 Types of Losses:

The machine loss consists of loss components in both stator and rotor parts. The losses, which affect on the machine overall efficiency are described in the following section.

3.6.1 Copper Loss

The copper losses in the stator winding can be calculated by,

$$P_{cu} = 3 * R_1 * I_a^2 \qquad \text{equ 3.8}$$

This loss can be calculated if the values of current and winding resistance are known at nominal load condition. The stator winding resistance per phase can be found by using the following equation:

$$R_1 = \frac{N_1 * l_{av}}{\sigma_{cu} * \pi * (0.5 * d_w)^2 * a_p * a_w} \qquad \text{equ 3.9}$$

Where,

N_1 is the number of turns per phase,

a_p is the number of parallel current path,

a_w is the number of parallel conductors.

The average length of the armature turn can be found by following equation,

$$l_{av} = L_i + l_{1in} + l_{1out} \qquad \text{equ 3.10}$$

Where,

l_{1in}= length of the inner end connection

l_{1out}= length of the outer end connection

3.6.2 Eddy Current Loss in the Winding

In coreless stator, the magnetic field produced by the PM through the conductor is changing with the relative position of the stator winding and rotor. This causes eddy current loss.

Eddy current loss occurs in the active portion of the winding and it is highly dependent on the wire diameter, magnetic flux density and frequency. The eddy current loss in the stator winding can be calculated by using the following expression:

$$P_e = \frac{\pi^2}{4} * \frac{\sigma_{cu}}{\rho_{cu}} * f^2 * d_w^2 * m_{con} * B_{mg}^2$$

equ 3.11

As it can be seen from equation 3.11, eddy current loss is heavily dependent on wire diameter. This means that a small reduction of wire diameter can reduce this loss by significant amount. In addition, for reduction of eddy current loss, Litz wire should be used. The stator winding is then splitted into parallel wires having smaller area of cross section instead of one thick conductor. It should be twisted in a way so that the geometry of each parallel conductor must result in the same length of coil.

3.6.3 Rotational or Mechanical Loss

The rotational losses are sum of the mechanical losses occurring in the bearing and the losses due to rotation of the rotor in air. This loss is the summation of friction losses, windage losses and ventilation losses.

$$P_{rot} = P_{fr} + P_{wind} + P_{vent}$$ equ 3.12

The friction losses in bearing can be calculated by using following expression:

$$P_{fr} = 0.06 * k_{fb} * (m_r + m_{sh}) * n$$

equ 3.13

Where,

m_r and m_{sh} is the mass of rotor and shaft in Kg.

n is the speed of the machine in rpm.

All the values are known to calculate the friction loss according to equation 3.13. The value of bearing friction coefficient, k_{fb} should be selected in the range of 1 to 3 m^2/s^2. For this design, the value of the constant coefficient has been chosen to 1 m^2/s^2.

The constant Reynold number for a given outer radius of the machine can be calculated by using the following formula:

$$R_e = \frac{2\pi n \rho R_{out}^2}{\mu}$$ equ 3.14

The other constant drag coefficient for turbulent flow can be calculated by:

$$c_f = \frac{3.87}{\sqrt{R_e}}$$ equ 3.15

The windage losses for a rotating disc of AFPM can be found:

$$P_{wind} = \frac{1}{2} c_f \rho (2\pi n)^3 (R_{out}^5 - R_{sh}^5)$$ equ 3.16

These losses are heavily dependent on outer radius of the machine, machine speed, resistivity and coefficient of drag.

Air-cooling is mostly used in AFPM machines. This machine has been designed without external cooling fan. For this reason, there is no ventilation loss for this design. So, $P_{vent} = 0$.

3.7 Efficiency:

The machine is a brushless motor with surface mounted PM arranged with Halbach array. After calculating all the losses, the total

electromechanical efficiency of the motor can be calculated by,

$$\eta = \frac{P_{out}}{P_{in}} * 100\ \% \qquad \text{equ 3.17}$$

Where,

$P_{out} = P_{elm} - P_{rot}$

$P_{loss} = P_{cu} + P_e + P_{rot}$

$P_{in} = P_{out} + P_{loss}$

Here, P_{out} is the mechanical output power.

3.8 Optimized Design Procedure:

The basic design was fine-tuned with the help of optimization algorithm. Machine designing is a non-linear process. Therefore, it is difficult to find out the optimum value of the parameters of the motor without any help of optimization algorithm. Optimization algorithm based on Matlab optimization tool is one of the advanced ways to find out the optimum value of the parameters.

3.8.1 Objective Function

The objective function of this design is to maximize the efficiency of the machine. Another objective function is to minimize the weight of the machine as well. These objective functions are highly dependent on the variables of the designed machine. In the tool, this objective function is written in m file which is a function of x vector containing the variable parameters x_1, x_2, …… x_n.

3.8.2 Optimization Tool for Analysis

In Matlab Optimization tool, there are several built in optimization algorithm. This optimization tool allows to select a solver, specify the options of optimization and finally the results are obtained by running the solver.

Among the solvers, *Fmincon* has been selected for running the optimization process.

The algorithm used for the optimization of motor design is Sequential Quadratic Programming (SQP) since SQP is an efficient algorithm for solving non-linear problems. [3]

Fmincon is a non-linear constraint solver that minimizes the optimization parameters starting at an initial estimate. [7]

Fmincon requires the definition of a set of lower and upper bounds for the design variables in vector x, so that the solution lies always in the range of $lb \leq x \leq ub$. [7]

Finally, a graphical interface allows to define the iteration method and the output parameters (variables to be optimized). The initial values of these parametres are also stated as this interface is dependent on the initial value of the variables.

3.8.3 Optimized Parameters and Ranges

There are six variables for this optimized design. These varying parameters are:

Number of Poles:

The pole number should be chosen in a way considering the effect on both copper loss and eddy current loss in the machine. The higher number of poles the higher magnetic flux density in the airgap according to equ 3.2. The average pole pitch of the machine is inversely proportional to the number of poles. The copper losses in the machine also decrease as the average length of stator turn decreases, which decreases stator resistance in the winding. However, the eddy current loss

increases with the increase in frequency. The number of poles of the machine has to be an even integer.

Magnet Length:

With the increase in magnet length, not only the weight of the machine increases but also the efficiency of the machine decreases. Since, the eddy current loss increases with the square of the magnetic flux density. The friction loss is dependent on the mass of the rotor core made of magnet. It effects on the loss of the machine. Thus, the overall efficiency of the machine decreases.

Stator Thickness:

Increase in stator thickness increases the effective air gap and axial length of the machine.

Diameter Ratio:

Diameter ratio is the ratio of input and output diameter of the machine. Increasing this parameter increases the copper losses of the machine with the increase in end winding length. However, the eddy current loss of the machine decreases with the reduction of conductor length of the machine.

Number of Parallel Wires:

The parallel wires having smaller cross sectional area as an alternative of thick conductor reduce eddy current loss.

Wire Diameter:

Wire diameter has a great influence on eddy current loss. Small reduction of diameter reduces this loss in significant quantity.

The range of the variables considered for this design is given in table 3.2:

Parameters	Range
Number of pole pair	8-50
Magnet length [m]	0.0004-0.02
Stator thickness [m]	0.0003-0.02
Diameter ratio	0.56-0.9
Number of parallel wires	1-20
Wire diameter [m]	0.00005-0.0010

Table 3.2: Range of variables

3.8.4 Optimization Results

The initial values of the parameters were obtained following the procedure described in appendix. There are some limitations associated with the Matlab Optimization tool. The optimization tool gives fractional values for the parameters, which is not acceptable for machine designing. To overcome this, a loop has been introduced in the m file to force the fractional values to the nearest integer. Another limitation is, as this tool is the minimizer, the objective function needs to be defined accordingly. For example, maximizing the efficiency $\boldsymbol{\eta}$ should be described as minimizing ($-\boldsymbol{\eta}$).

The first problem definition did not give satisfying results. Therefore, the definition was improved according to the following description.

Step 1:

The fill factor of the machine should be in the range of 0.4-0.6. The Matlab optimization tool always set the variable to the upper limit. Practically, it is not possible to have high fill factor. For this design, it was then assumed as constant and equal to 0.5. In this way, the insulation of the conductor is considered.

Step 2:

The number of turns of the machine was first considered as a variable. The obtained number of optimum turns was found to be within the upper limit of the set range. In addition, this caused the other parameters to be optimized towards their lower limits. Hence, the design was not realistic. To avoid this problem, the number of turns was not kept as a variable. It was calculated according to equation 3.6.

Step 3

To calculate the flux density using Halbach arrangement, equation 3.2 has been used initially. But, leakage flux is not taken into account with this equation. Hence, equation 3.3 has been used that considers the leakage flux. The observed variation of flux led to a more realisitic case.

Step 4

Neglecting friction loss gives an electrical efficiency of 99% at the cost of high magnet mass. The values of the variables are shown in table 3.3.

Parameter	Value
Number of pole pair	10
Magnet length [m]	0.02
Stator thickness [m]	0.0184
Diameter ratio	0.56
Number of parallel wires	4
Wire diameter [m]	0.0001

Table 3.3: Primary obtained parameters without considering frictional loss

With the value of the parameter from table 3.2, the magnet mass of the machine becomes 16 kg. Thus, the total weight of the machine becomes 24 kg with 99% efficiency.

Since with friction loss, the overall efficiency of 97% with a decreased magnet mass was obtained. Hence, friction loss has been taken into account while optimizing.

Step 5

Initially conisdering the parameters *wire diameter* and *number of parallel wires* as variable gave unrealistic results while optimizing. To eliminate this problem, the area of copper was first calculated. The stator resistance can be calculated from the obtained copper area. Finally, optimized parameters were obtained considering the above stated parameters as variables keeping the area of the copper the same.

Step 6

Litz wire has a great impact on reducing eddy current loss. With the use of Litz wire, it has been assumed that eddy current loss is 5% of the copper loss. With this assumption, the wire diameter does not have a great influence on eddy current loss any more. It was not considered anymore as a variable and was calculated by following equation 3.18 instead.

$$d_w = \sqrt{\frac{kfn_c t_w w_s}{a_p a_w N_1}} \qquad \text{equ 3.18}$$

This gave the value of $d_w = 0.8\,mm$

The final optimum values of the varying parameters are shown in table 3.4.

Parameter	Value
Number of pole pair	24
Magnet length [m]	0.008
Stator thickness [m]	0.0087
Diameter ratio	0.785
Number of parallel wires	4

Table 3.4 Optimum Values of Parameters

With the values of these parameters, the characteristics of this design in table 3.5 were obtained:

Geometrical parameters	***Value***
Outer diameter [m]	0.315
Inner diameter [m]	0.247
Axial length of machine [m]	0.0327
Radial length of PM [m]	0.0339
Number of coil sides, S1	144
Magnet spacing [m]	0.0107
Number of turns, N_1	192
Fill factor, k_f	0.5
Torque constant, k_T [Nm/A]	2.3960
Airgap length along each side,g [m]	0.001
Remanent flux density of magnet [T]	1.33

Electrical losses	***Value***
Current, I_a [A]	1.46
Resistance, R_1 [Ω]	0.17
Copper loss, P_{cu} [W]	1.13
Magnetic flux density(surface of magnet) [T]	0.8919
Magnetic flux density(middle of copper) [T]	0.6164
Eddy current loss, P_e [W]	0.0567

Mechanical losses	***Value***
Friction loss, P_{fr} [W]	1.6012
Windage loss, P_{wind} [W]	0.0288
Ventilation loss, P_{vent} [W]	0
Total Mechanical loss, P_{rot} [W]	1.63

Parameter	***Value***
Total loss, P_{loss} [W]	2.8199
Output power, P_{out} [W]	99.1627
Input power, P_{in} [W]	101.9827
Efficiency, η [%]	97.23

Weight	***Value***
Magnet mass [Kg]	3.68
Conductor mass [Kg]	1.1449
Mass of rotor [Kg]	1.4087
Total weight [kg]	6.24

The obtained machine will run at an operating frequency of 110 Hz using a commercial frequency converter.

The several statges of the design are depicted in figure 16:

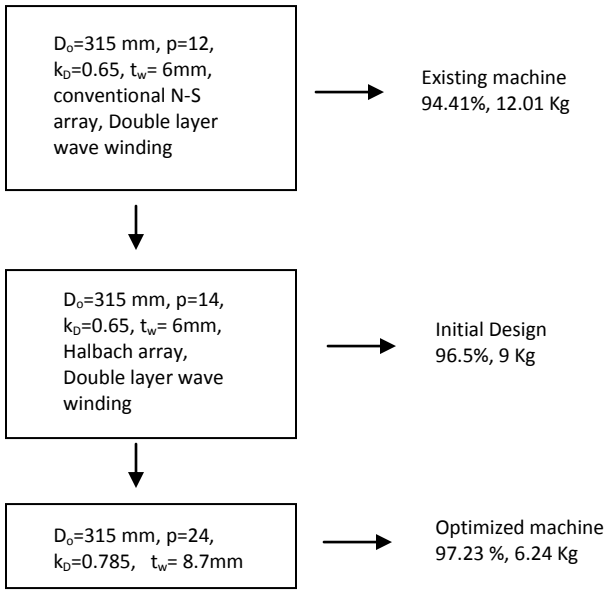

Fig 16: Design improvement stages

Chapter 4 FEM Analysis

4.1 Background on Comsol Multiphysics 4.1

The goal of computer simulation is to facilitate adaptation of a model and display characteristics same as real time scenario.

Finite Element Method (FEM) is one of the techniques to find an approximate solution closer to the real time scenario. FEM does the point-by-point analysis, which gives results that are more precise compared to analytical calculation in several aspects.

COMSOL multiphysics [14] is one of the flexible platform which allows to model all relevant features of the design. It brings a level of simplicity on the simulation work with the help of organized based model and streamlined model building process.

COMSOL Multiphysics 4.1 is one of the latest versions available of the software, which has been used in this analysis. This version has introduced a new model builder. This provides the dynamic control of the simulation process.

4.2 Process of COMSOL Multiphysics

In order to get accurate results with the help of Comsol Multiphysics 4.1, all the steps have to be executed properly.

Firstly, the model has been built by model tree. The design of whole machine is not necessary here. One pole pitch of the machine has been drawn to find out the values of magnetic flux density in the airgap, induced voltage, and torque.

Secondly, from the material browser, all the materials, which were used in the design, have been stated.

After defining the design and the materials, all the boundary conditions have been selected. Now the design is ready for mesh building. The simplest way of meshing is to create an unstructured tetrahedral mesh. Several mesh sequences can also be created.

Finally, after solving the defined problem, all the results and necessary plots can been obtained.

4.3 Results

The step time has been chosen in such a way so that the simulation runs for three periods. The total simulation time is,

$$T_{simulation} = \frac{3}{f} = \frac{3}{110} = 0.027\ s$$

100 time-steps have been considered per calculation. The time-period for one single step is:

$$T_{step} = \frac{0.027}{100} = 0.00027\ s$$

The last time-step is calculated for, $t = 0.027\ s + 0.00027\ s = 0.02727\ s$

4.3.1 Magnetic Flux Density

Figures 17 and 18, illustrate the 2D FEM results of the ironless AFPM. The remanent flux density of the rare magnet NdFeB was set to 1.33 T. The thickness of coreless stator winding was 8.7 mm. The axial height for each PM material was assumed to be 8 mm and the thickness of airgap for each side was taken into account as 1 mm.

One pole pair of the machine was considered for acquiring the estimated diagram. Figure 17 presents the 2D view of colour plot of magnetic flux density B with the iso values curve of potential vector.

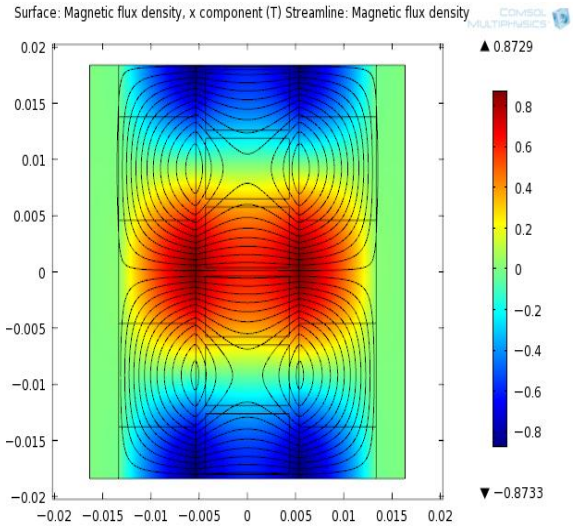

Fig 17: Magnetic flux density

Figure 18 represents the flux tubes on their own. Here, the flux line passing between the magnets to airgap can be seen.

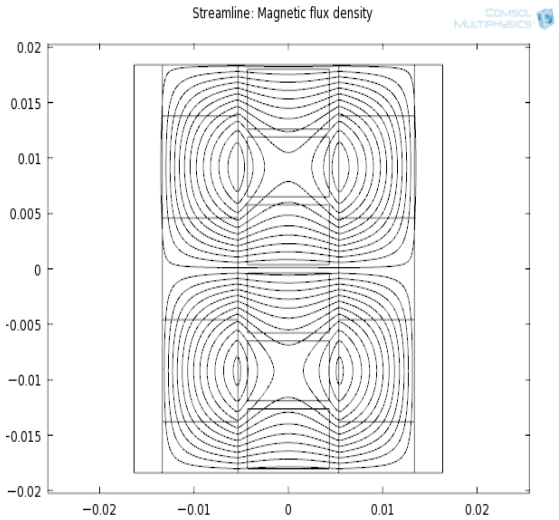

Fig 18: Equi Potentials

Figure 19 shows the value of magnetic flux density at the surface of Halbach array. Its maximal value is 0.858 T. In Comsol, a line was plotted along the active surface of the halbach array. The peak value obtained from analytical calculation was 0.8919 T. There is a minor difference in between the results from FEM and analytical calculation which is 3.8 %.

In FEM analysis, a general wave function has been considered for demonstrating the motor as rotating machinery.

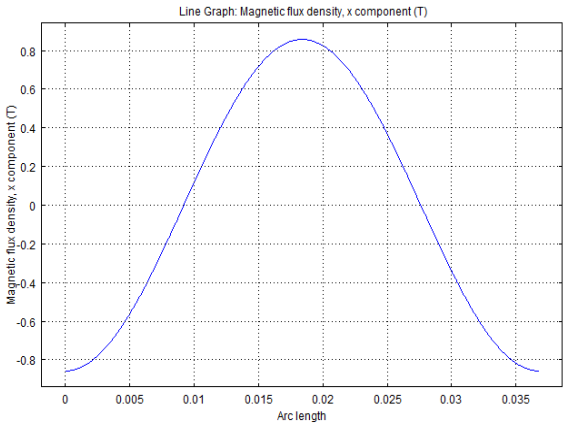

Fig 19: Magnetic flux density in the airgap at the surface of Halbach array

Figure 21 illustrates the magnetic flux density in the middle of copper. To obtain the value from FEM analysis, a line was defined in the middle of the stator.

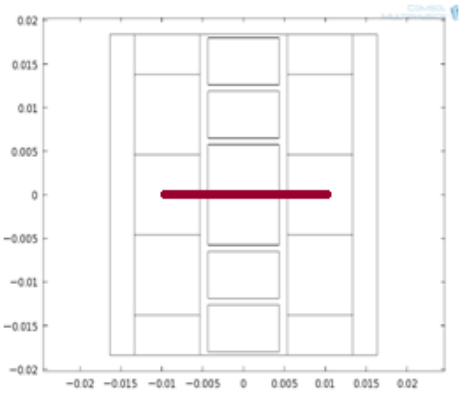

Fig 20: Cut line at the point -0.01 to 0.01 at X axis with the value of 0 at Y axis

It can be seen from the curve that, the flux density is increasing in the beginning, reaches the peak value and after that at the average of copper, it is decreasing. This is according the equation used in analytical calculation. The value obtained in FEM analysis is 0.603 T whereas, the value is 0.6164 T in analytical calculation. The difference between the analytical calculation and FEM simulation is 2 %.

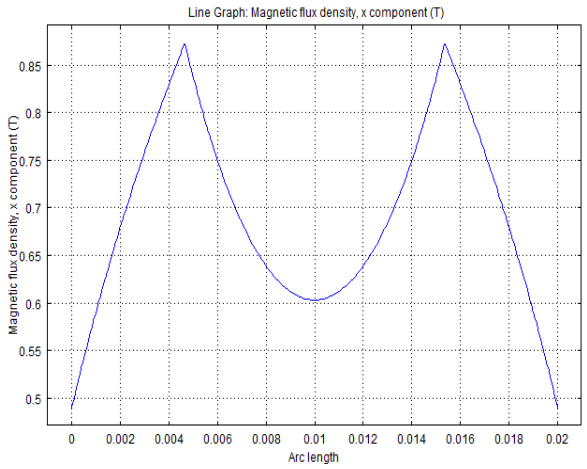

Fig 21: Flux density in the middle of the stator

The values of the flux density with the support of Halbach array was obtained by using Comsol Multiphysics 4.1, which has lower value than the value from analytical calculation.

4.3.2 Induced Voltage

The induced voltage in the coils can be obtained when there is no current flow in the stator winding. The voltage induced in the coil is equal to the time variation of magnetic flux linkage.

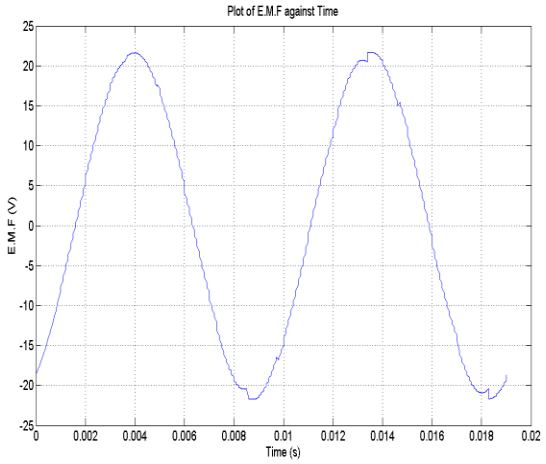

Fig 22: Plot of EMF vs Time

Figure 22 shows the induced voltage at no-load condition at 278 rpm.

The fundamental component of the induced voltage obtained from FEM is 21.3 V. The analytical value of induced voltage is 23 V. The difference is 7.39 %.

4.3.3 Torque

The electromagnetic torque for a coreless AFPM is calculated on basis of Lorentz force theorem. This occurs due to interaction of current carrying conductor with the magnetic field created by the PM material.

Figure 23 illustrates the amplitude of Lorentz force density in the simulated geometry.

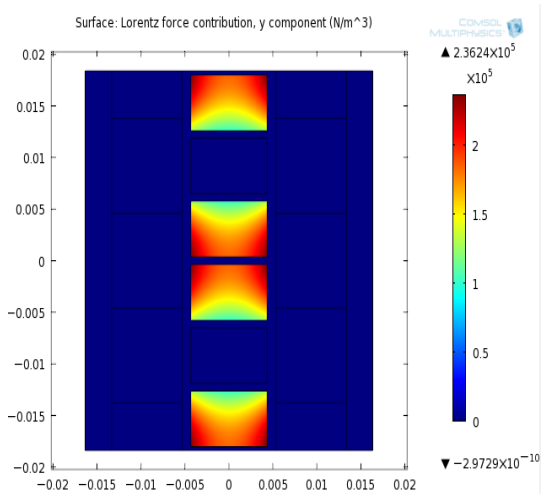

Fig 23: 2D view of force density

Figure 24 shows the peak value of the torque at nominal condition obtained from FEM analysis. Its mean value is 31.53 Nm.

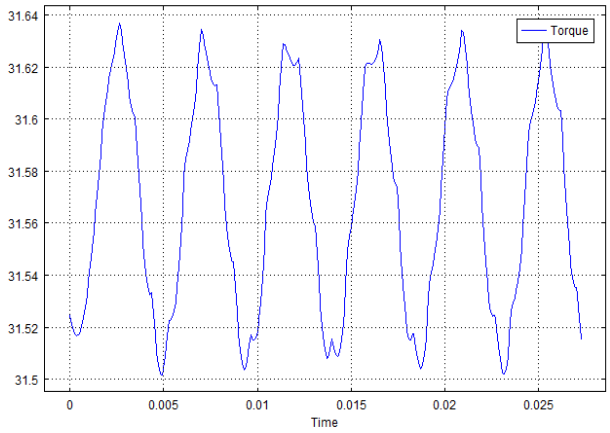

Fig 24: Torque vs Time

The percentage change between the minimum and maximum value of torque is 0.09 %.

4.4 Conclusion

In this chapter the results obtained from the analytical calculations have been compared with the one's obtained by FEM analysis. The results are found similar as shown in table 4.1.

	Analytical Result	FEM simulation	# in %
Induced voltage	23 V	21.3 V	7.39 %
Flux density (at surface)	0.8919 T	0.858 T	3.8 %
Flux density (at the middle of stator)	0.6164 T	0.603 T	2.17 %

Table 4.1: Comparison of results

Chapter 5 Discussion

5.1 Discussions on Obtained Results:

The parameters of the existing machine i.e pole number of the machine, magnet length, stator thickness, diameter ratio, number of turns, wire diameter, number of parallel wire have been obtained with the help of optimization tool to attain a high efficiency low weight motor.

The design uses Litz wire because it allows significant reduction of eddy current losses. However, Litz wires are expensive.

Increase in pole number increases the electrical frequency. Thus, iron loss of the machine increases. Therefore, ironless stator has been considered for eliminating the iron losses of the machine.

The N-S magnet arrangement has been replaced by the Halbach array. Halbach array provides more sinusodal magnetic flux density with less harmonic distortion. With the aid of Halbach arrangement, it was not necessary to use iron in the rotor back. Thus, this reduced the weight of the machine.

The overall efficiency of the machine is 97.2 % with a weight of 6.24 Kg. The optimized design presents improved performance compared to the existing machine as shown in table 5.1.

	Old design	***New design***	***# in %***
Total loss	5.68 W	2.8226 W	-50.3%
Machine weight	12 Kg	6.2 Kg	-48.3 %
Efficiency	94.41 %	97.2 %	2.87 %

Table 5.1 Comparison of designs

5.2 Future Work

As future work in this project, it is suggested to focus on the stator design. Different types of winding layout with coil arrangement should be taken in consideration. The effect of lap winding on the overall performance of the machine should be analysed.

The developed procedure used for optimization process should be improved, as the process is dependent on the initial conditions.

It has been assumed that the eddy current loss is 5% of copper loss because of use of Litz wire. Since this is an estimated loss percentage, a more accurate value should be calculated and results analyzed.

The fill factor for this design was assumed to be. The highest realistic fill factor with Litz wire should be investigated. This is a significant task for further improvement of the machine, as it is important to increase the overall efficiency of the machine.

Improvements should also focus over energy storage capacities and inverter efficiency at system level.

Appendix A

The existing machine has the following parameter values [2]:

$p = Number\ of\ Pole\ Pair = 12$

$h_m = Magnet\ Length = 12\ mm$

$g = Airgap\ Length = 2\ mm$

$N_1 = Number\ of\ Turns = 96$

$t_w = Winding\ Thickness = 6\ mm$

$D_o = Outer\ Diameter = 315\ mm$

$t = Magnet\ Spacing = 10\ mm$

$B_g = Magnetic\ Flux\ Density = 0.776\ T$

$Type\ of\ Winding$:

$Double\ Layer\ Wave\ Winding$

$Type\ of\ Magnet\ Arrangement$:

$Conventional\ N-S$

$Efficiency = 94.41\ \%$

$Total\ Weight = 12.01\ Kg$

The parameter values of initial design were as follows:

$p = Number\ of\ Pole\ Pair = 14$

$h_m = Magnet\ Length = 10\ mm$

$g = Airgap\ Length = 3\ mm$

$N_1 = Number\ of\ Turns = 98$

$t_w = Winding\ Thickness = 6\ mm$

$D_o = Outer\ Diameter = 315\ mm$

$t = Magnet\ Spacing = 12\ mm$

$B_g = Magnetic\ Flux\ Density = 0.84\ T$

$Type\ of\ Winding$:

$Double\ Layer\ Wave\ Winding$

$Type\ of\ Magnet\ Arrangement$:

$Halbach\ Array$

$Efficiency = 96.5\ \%$

$Total\ Weight = 9\ Kg$

Calculation the Machine Parameters Based on Final Design:

All the equations used for the calculation have been taken from the book [1].

Magnetic Flux:

$$\phi_f = \frac{1}{8p}\alpha_i B_{mg}\pi D_o^2(1-k_D^2)$$

$$= 2.44 * 10^{-4}\ Wb$$

Maximum Stator Width:

$$w_s = \frac{\pi D_i}{s_1}$$

$$= 0.0054\ \mathrm{m}$$

Length of the Conductor:

$$L_i = \frac{1}{2} * (D_o - D_i)$$

$$= 0.0339\ m$$

Length of Inner End Connection:

$$l_{inner} = \left(\frac{\omega_c}{\tau_c}\right) * pi * \frac{D_i}{2 * p}$$

$$= 0.0162\ m$$

Length of Outer End Connection:

$$l_{outer} = l_{inner} * \left(\frac{D_o}{D_i}\right)$$

$$= 0.0206\ m$$

Thus, the average length of the armature turns,

$$l_{av} = L_i + l_{inner} + l_{outer}$$

$$= 0.1445\ m$$

Reynold Number:

$$R_e = \frac{2\pi n \rho R_{out}^2}{\mu}$$

$$= 4.76 * 10^4$$

Drag Coefficient:

$$c_f = \frac{3.87}{\sqrt{R_e}} = 0.0177$$

Average Pole Pitch:

$$\tau = \frac{\pi D}{2p}$$

$$= 0.0184\ m$$

Area of Copper:

$$A_{cu} = \frac{\tau t_w}{3N_{ct}} * k_f$$

$$= 3.34 * 10^{-6}\ m^2$$

Calculation of Inductance:

Considering, $\mu_{ref} \approx 1$

$$g' = 2[(g + 0.5t_w) + \frac{h_m}{\mu_{ref}}]$$

$$= 0.0267\ m$$

Armature reactance of d axis and q axis are equal and $k_{fd} = k_{fq} = 1$

The q axis and d axis inductance are equal.

$$L_{ad} = L_{aq}$$

$$= \frac{m_1\ \mu_0}{\pi}\left(\frac{N_1 k_{w1}}{p}\right)^2 \frac{(R_{out}^2 - R_{in}^2)}{g'}$$

$$= 27\ \mu H$$

Since, it is difficult to acquire accurate equation for λ_{1s} of coreless machine,

it is assumed that,

$$\lambda_{1s} = \lambda_{1e} = 0.3q$$

$$l_{1e} = 0.5(l_{inner} + l_{outer})$$

$$= 0.0184\ m$$

Leakage Factor:

$$\tau_{d1} = \frac{\pi^2(10q^2 + 2)}{27}\sin\left(\frac{30^0}{q}\right) - 1$$

$$= 1.19$$

Specific Permeance for Differential Leakage Flux:

$$\lambda_{1d} = \frac{m_1 q \tau k_{w1}^2 \tau_{d1}}{\pi^2 g' k_{sat}}$$

$$= 0.25$$

Leakage Inductance:

$$L_1 = 2\mu_o \frac{N_1^2 L_i}{pq}(\lambda_{1s} + \frac{l_{1e}}{L_i}\lambda_{1e} + \lambda_{1d})$$

$$= 60\ \mu H$$

Thus the stator inductance $= L_1 + L_{ad}$

$$= 87\ \mu H$$

Number of Conductor per Slot

$$N_c = \frac{a_p a_w N_1}{pq}$$

$$= 32$$

The Torque-Speed Characteristic in a Simplified Form:

$$\frac{n}{n_o} = 1 - \frac{I_a}{I_{ash}} = 1 - \frac{T_d}{T_{dst}}$$

$$n_o = no\ load\ speed = \frac{V_{dc}}{k_E}$$

$$I_{ash} = Locked\ rotor\ armature\ current$$

$$= \frac{V_{dc}}{R}$$

Where, R = R_1 for half wave operation

and R=2 R_1 for full wave operation.

$$T_{dst} = Stall\ torque$$

$$= k_{Tdc} I_{ash}$$

Thus, the value of no load speed with the assumption of linear torque-speed curve is 278 rpm.

Appendix B

Figure 25 presents the magnet dimensions for the motor.

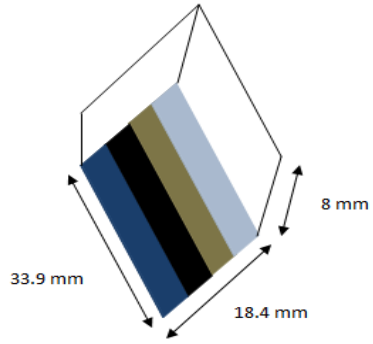

Fig 25: Magnet Dimensions with 90^0 (n_m=4) Halbach array

The colours are indicating the number of PM pieces.

Radial length of PM = 33.9 mm

Average length of pole pitch= 18.4 mm

Axial length of PM= 8 mm

Figure 26 presents the dimention of stator slot. Here, in the double layer winding two sides of coil coils are accommodate in the slot. The number of parallel wires is 4.

Stator thickness=8.7 mm

Slot width= 5.4 mm

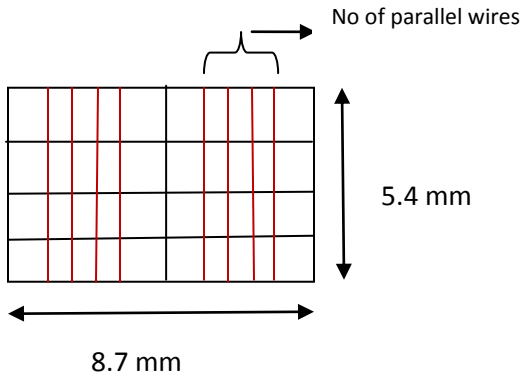

Fig 26: Stator Slot Dimentions

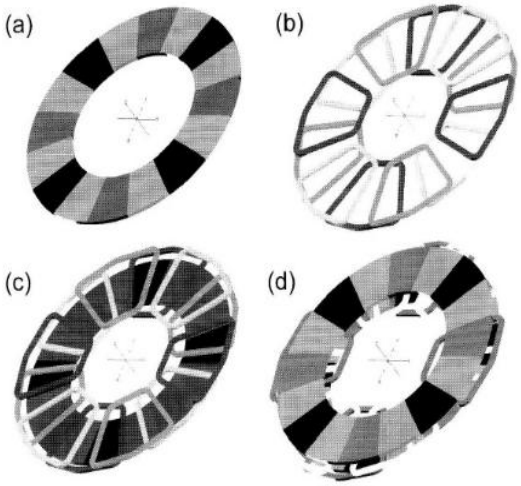

Fig 27: A construction of a three phase, 8 pole AFPM brushless machines with PMs arranged in Halbach array: (a) PM ring (b) stator winding (c) one half of the twin rotor (d) stator winding and complete twin rotor [1]

Figure 28 presents the flux path for single stator, double rotor AFPM machine.

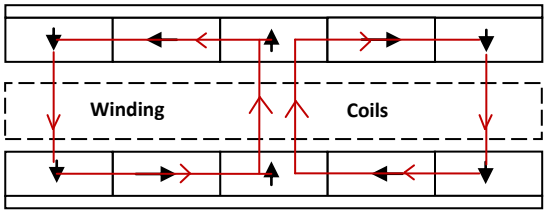

Fig 28: Three Phase winding, PM polarities and magnetic flux paths of double-sided disc machine with one coreless stator

Acknowledgements

I am heartly thankful to my supervisor Prof Robert Nilssen at NTNU for his suggestions and guidelines on machine designing. His encouragement also facilitated the development of my understanding of the subject area. I will never forget the inspiration provided by Robert Nilssen, which helped me to overcome the obstacles during my thesis work.

I would also like to thanks Zhaoqiang Zhang at NTNU for helping me in the area of Comsol Multiphysics. His ideas on Comsol Multiphysics related to machine designing has helped me to bring out the desired result.

I am also thankful to Fedrik Viholve Endresen for his help on winding arrangement.

I am also thankful to the all team members of DNV Fuel Fighter.

Last but not the least, I would like to thank Associate Prof Juliette Soulard at KTH for giving me the permission for this thesis work and encouraging me as well.

I would also like to thanks to my friends, family members and well-wishers.

Lubna Nasrin
October 2011
Stockholm, Sweden

References

1. Jacek F. Gieras, Rong-Jie Wang and Maarten J. Kamper , '*Axial Flux Permanent Magnet Brushless Machines',* Kluwer Academic Publishers (2004).

2. Andre Dahl-Jacobsen , '*Energy Efficient Motor for Shell Eco Marathon*', Master Thesis, NTNU, Norway, July 2010.

3. Florence Libert, '*Design, Optimization and Comparison of Permanent Magnet Motors for a Low-Speed Direct-Driven Mixer*', Licentiate Thesis, Royal Institute of Technology, Stockholm, 2004.

4. F.G Rossouw, '*Analysis and Design of Axial Flux Permanent Magnet Wind Generator System for Direct Battery Charging Applications*', Master Thesis, Stellenbosch University, South Africa, March 2009.

5. H Kierstead, R-J Wang and M J Kamper, '*Design Optimization of a Single Sided Axial Flux Permanent Magnet In-Wheel Motor with Non-Overlap Concentrated Winding*', University of Stellenbosch, Department of Electrical and Electronic Engineering, Stellenbosch, South Africa.

6. Adel El Shahat, Ali Keyhani and Hamed El Shewy, '*Micro-Generator Design for Smart Grid System (Comparative Study)*, International Journal on Smart Sensing and Intelligent Systems Vol. 3, No. 2, June 2010

7.http://www.mathworks.se/help/toolbox/optim/ug/fmincon.html

8. H. C. Lovatt, V.S. Ramsden, B.C. Mecrow '*Design of an In Wheel Motor for a Solar-Powered Vehicle*', IEEE Proc Elecr. Power Appl, Vol. 145, No. 5, September 1998.

9. Federico Caricchi, Fabio Crescimbini, Onorata Honorati, Giulia Lo Bianco, Ezio Santini, ' *Performance of Coreless Winding Axial Flux Permanent Magnet Generator with Power Output at 400 Hz, 3000 r/min*', IEEE Industry Applications Society Annual Meeting, Vol. 34, No. 6, November/December 1998.

10. Funda Sahin, '*Design and Development of a High-Speed Axial-Flux Permanent Machine*', Phd Thesis, Technische Universiteit Eindhoven, 2001. Proefschrift. - ISBN 90- 386-1380-1,NUGI 832

11. M. Aydin, S. Huang and T.A. Lipo, '*Axial Flux Permanent Magnet Disc Machines: A Review*',Research Report 2004-10, Wisconsin Electric Machines and Power Electronics Consortium.

12. Seyed Mohsen Hosseini, Mojtaba Agha-Mirsalim and Mehran Mirzaei, '*Design, Prototyping, and Analysis of a Low Cost Axial-Flux Coreless Permanent-Magnet Generator*' IEEE Transactions on Magnetics, Vol. 44, No. 1, January 2008.

13. Astrid Røkke,'*Improvement of Axial Flux Permanent Magnet Machine using Halbach Arrays*', Project Work, NTNU, Trondheim, 2006.

14.http://www.shell.com/home/content/ecomarathon/europe/for_participants/europe_rules/

15. http://www.comsol.com/

List of symbols

Symbols	Names	Units
D_o	Outer Diameter of Rotor	m
D_i	Inner Diameter of Rotor	m
k_D	Diameter Ratio	
K_{w1}	Winding Factor	
T_d	Electromagnetic Torque	Nm
k_E	Voltage Constant	V/rpm
p	Number of Pole Pairs	
S_1	Number of Slots	
w_s	Stator Width	m
n	Speed	rpm
f	Frequency	Hz
ρ_{cu}	Resistivity of Copper	Ωm
σ_{cu}	Conductivity of Copper	S/m
l_{1av}	Average Length of the Turn	m
P_{cu}	Copper Loss	W
P_e	Eddy Current Loss	W
P_{wind}	Windage Loss	W
P_{fr}	Friction Loss	W
P_{vent}	Ventilation Loss	W
L_i	Length of Conductor	m
h_m	Axial Length of PM	m